Research Article | Vol. 14, No. 7 / 1 Jul 2023 / Biomedical Optics Express 3654
Biomedical Optics EXPRESS

Spatiotemporal defocus sensitivity function of the human visual system

VICTOR RODRIGUEZ-LOPEZ,[1,*] WILSON GEISLER,[2] AND CARLOS DORRONSORO[1,2,3]

[1] Institute of Optics, Spanish National Research Council (IO-CSIC), IO-CSIC, Serrano 121, E-28006, Madrid, Spain
[2] Center for Perceptual Systems, The University of Texas at Austin, 1 University Station, A8000, E-78712, Austin, Texas, USA
[3] 2EyesVision SL, Plaza de la Encina, 10, núcleo 3, planta 4ª, E-28760 Tres Cantos, Madrid, Spain
[*] victor.rl@io.cfmac.csic.es

Abstract: Tunable lenses make it possible to measure visual sensitivity to rapid changes in optical power, surpassing the limits imposed by mechanical elements. Using a tunable lens system, we measured, for the first time, the spatiotemporal defocus sensitivity function (STDSF), and the limits of human defocus perception. Specifically, we measured defocus sensitivity using a QUEST adaptive psychophysical procedure for different stimuli (Gabor patches of different spatial frequencies, natural images, and edges) and we developed descriptive models of defocus perception. For Gabor patches, we found on average (across seven subjects) that the maximum sensitivity to defocus is 0.22 D at 14 cpd and 10 Hz, and that the upper limits of sensitivity are 40 cpd and 40 Hz. Our results suggest that accommodation remains fixed while performing the defocus flicker-detection task. These results have implications for new technologies whose working principles make use of fast changes to defocus.

1. Introduction

There is a long history of research regarding the spatiotemporal properties of the human visual system. This research has provided a useful description of our limits of visibility, as well as invaluable fundamental scientific knowledge about vision [1–4]. The spatial contrast sensitivity function (SCSF), known as CSF in the scientific literature, defines the sensitivity to spatial modulation in contrast, i.e., the minimum contrast visible for different spatial frequencies. The typical SCSF is a curve with maximum sensitivity between 1-2 cycles per degree (cpd), and falling more rapidly in high than in low spatial frequencies [5,6]. Common cutoff spatial frequencies, i.e., the maximum spatial frequency visible at maximum contrast (contrast 1), lie between 30 and 40 cpd.

On the other hand, the perception of temporally modulated contrast is described in the temporal contrast sensitivity function (TCSF) [1,4]. When observing an object periodically changing over time, the visual system might perceive said temporal change (flicker) or not (fusion). The TCSF curve is similar to the SCSF, although in the temporal domain. The maximum of the TCSF is found at around 10 cycles per second (Hz), falling more rapidly for high than for low temporal frequencies, similar to the SCSF. The cutoff temporal frequency that defines the perceptual boundary between flicker and fusion is known as the contrast critical flicker frequency (CFF). The CFF is well known to be around 50-70 Hz, depending on the characteristics of the stimulus such as luminance, size, spatial frequency content, and retinal eccentricity, among others [4].

The SCSF and the TCSF can be combined in the spatiotemporal contrast sensitivity function (STCSF), which defines what is visible, at the same time, in the spatial and temporal domains. Robson [2] measured the STCSF for the first time, studying the contrast thresholds of a stimulus for different spatial and temporal frequencies. The limits of spatiotemporal perception define the

#486242 https://doi.org/10.1364/BOE.486242
Journal © 2023 Received 9 Feb 2023; revised 31 May 2023; accepted 1 Jun 2023; published 26 Jun 2023

Biomedical Optics EXPRESS

'window of visibility' [7], a region of the spatiotemporal domain that determines the limits for the perception of visible and fused images.

Contrast sensitivity has been extensively described both in the spatial and temporal domains because contrast is a fundamental feature in visual perception. Another important feature of vision is defocus. Defocus can be considered as a contrast modulation but with a different effect for different spatial frequencies [8]. Essentially, defocus attenuates high spatial frequencies more than mid and low spatial frequencies, and as the amount of defocus increases, more high frequencies are removed [9].

Some studies have measured the sensitivity to temporal changes in defocus, although only at low temporal frequencies [10–16]. For example, Walsh et al. [15] found that the minimum threshold of 0.1 D occurred for low spatial frequency stimuli, although their hardware limited the temporal frequency to a maximum of 4 Hz. Mathews et al. [16] also measured the sensitivity to temporal changes of defocus, but for even lower temporal frequencies (from 0.2 to 0.8 Hz) and fixed peak-to-valley defocus changes of 0.5 D and 2.0 D. Other studies have evaluated the perception of changes in onscreen blur, by computationally manipulating digital images [17]. However, a complete study of the temporal sensitivity to defocus, including higher temporal frequencies, has not been addressed due to considerable limitations in the mechanical hardware needed to make rapid temporal changes in optical defocus.

Fortunately, modern technologies such as tunable lenses allow fast and precise changes in optical power, overcoming the limitations of traditional setups. Tunable lenses are widely used in the field of artificial vision [18], where temporal changes of the focus plane are often needed. Autofocus systems are a representative example. Other emerging technologies use tunable lenses to induce periodic defocus variations. SimVis Gekko [19] uses a temporal multiplexing approach to simulate multifocal ophthalmic corrections by superimposing several images corresponding to different optical powers. If the temporal frequency is high enough, the multifocal image is perceived as static. At the temporal frequency used for temporal multiplexing, 50 Hz, no flicker perception is expected. Additionally, a new subjective refraction method to estimate the refractive error of an eye (i.e., myopia, hyperopia, and astigmatism), called Direct Subjective Refraction, produces defocus flicker cues on purpose at 15 Hz, to guide the estimation of the refractive error [20]. These novel technologies invite further investigation of the spatiotemporal aspects of defocus sensitivity.

As mentioned, previous studies regarding temporal sensitivity to defocus were incomplete due to hardware limitations that prevented measurements at high temporal frequencies. These limitations were overcome by tunable lenses, which allowed the development of novel technologies and applications in the field of ophthalmology and optometry that use temporal defocus changes as their working principle. Thus, the main goal of this study is to investigate the response of the visual system to changes in defocus for different temporal and spatial frequencies and natural and artificial stimuli. We performed experimental measurements of the temporal defocus sensitivity function (TDSF) and the spatial defocus sensitivity function (SDSF), and we combine both in the spatiotemporal defocus sensitivity function (STDSF), described for the first time. We used consolidated models in contrast perception to describe these defocus sensitivity functions. We also investigated the impact of accommodation in the measurement of the TDSF.

2. Methods

In this study, we measured the spatiotemporal defocus sensitivity function (STDSF), using a tunable lens inducing sinusoidal temporal defocus waves. A two-interval forced-choice (2IFC) paradigm, implemented in an adaptive QUEST psychophysical algorithm, was used to determine the threshold in peak-to-valley defocus change, for several temporal frequencies and spatial frequencies.

Biomedical Optics EXPRESS

2.1. Observers

Seven observers participated in the experiment, aged from 22 to 28 years old (25 ± 2.6 on average). All of them had healthy stereovision (<40 arc seconds) and no color vision abnormalities. Their maximum visual acuity with their current prescription, measured with standard optometry techniques, was 0.0 logMAR or higher. Observers performed the experiments wearing their usual ophthalmic prescription, if any. Three of the observers wore contact lenses, two wore glasses and two did not need any optical compensation. Only the left eye was measured.

2.2. Experimental setup

A tunable lens, able to modify its optical power in response to an electric signal, is the active element generating sinusoidal temporal defocus waves with different peak-to-valley defocus changes and temporal frequencies. To compensate for the dioptric distance to the display, the center of the wave was always 1.0 D, thus the defocus of the wave (in diopters) changed sinusoidally around 1.0 D (Fig. 1(A)). We used a liquid-membrane tunable lens (EL-10-30-TC, Optotune, Switzerland) that enables accurate variations in optical power in temporal regimes up to 100 Hz [18]. The tunable lens is optically projected onto the pupil plane of the observer's eye via a 4f-projection optical system (Fig. 1(A)). The physical distance from the eye's pupil to the first lens is 45 mm, and from the tunable lens to the screen is 1 m. While the actual distance from the pupil of the eye to the monitor is 1.25 m, the effective optical distance is 1 m. The tunable lens is carefully calibrated in static and dynamic optical power and temperature variations according to previous work [18,21–23], to confidently induce the intended optical power (defocus) variations [18–25]. This optical setup allows changes in retinal blur (defocus) without displacements nor changes in magnification. A variable diaphragm located next to the tunable lens was also projected onto the pupil of the observer to allow changing the pupil diameter of the eye.

The stimulus was displayed on an EliteDisplay E240 23.8'' monitor (HP Inc, Palo Alto, USA) with a size of 55.72 × 34.22 cm, a spatial resolution of 1920 × 1080 pixels, and a refresh rate of 60 Hz. The maximum luminance of the monitor was 250 cd/m^2. The monitor was driven by an NVIDIA Quadro P4000 dual Graphic card.

The position of the subject was stabilized with a bite bar. Subjects aligned themselves in X and Y axes with the entrance pupil of the optical system using a micrometric system, a square defocus wave of 0 and 2 D peak-to-valley at 15 Hz, and a white, thin, and large cross over a gray background as an alignment stimulus. The alignment task is finding the XY position of the pupil producing minimum flicker displacement (maximum superposition between images for the two optical powers), corresponding to the alignment of the optical axis of the projection system to the pupil entrance of the subject.

2.3. Stimuli

Seven gray-scale stimuli were used during the experiments, all of them centered in a square window subtending 4 degrees of visual field. (Figure 1(B)). Stimuli 1-5 were Gabor patches of 2, 4, 8, 16, and 32 cpd, which are equally spaced in a logarithmic scale of spatial frequency. The standard deviation of the Gabor patch was 0.48 degrees in X and 0.44 degrees in Y. We used constant-cycle Gabor patches as they are used to model receptive fields, as base functions in wavelets modeling ideal observers, or image understanding, and are potentially more useful than constant-degree functions (Gabors) to mimic real work performance. To approach these measurements to real-world stimuli, stimulus 6 was selected from a natural images database [26] of well-focused images with a 1/f^2 frequency spectrum and the same contrast and luminance, that contained fruits, vegetables, bushes, and trees, and. Stimulus 7 was a Gaussian edge, which contains all spatial frequencies and can be considered the most artificial stimuli compared to

Biomedical Optics EXPRESS

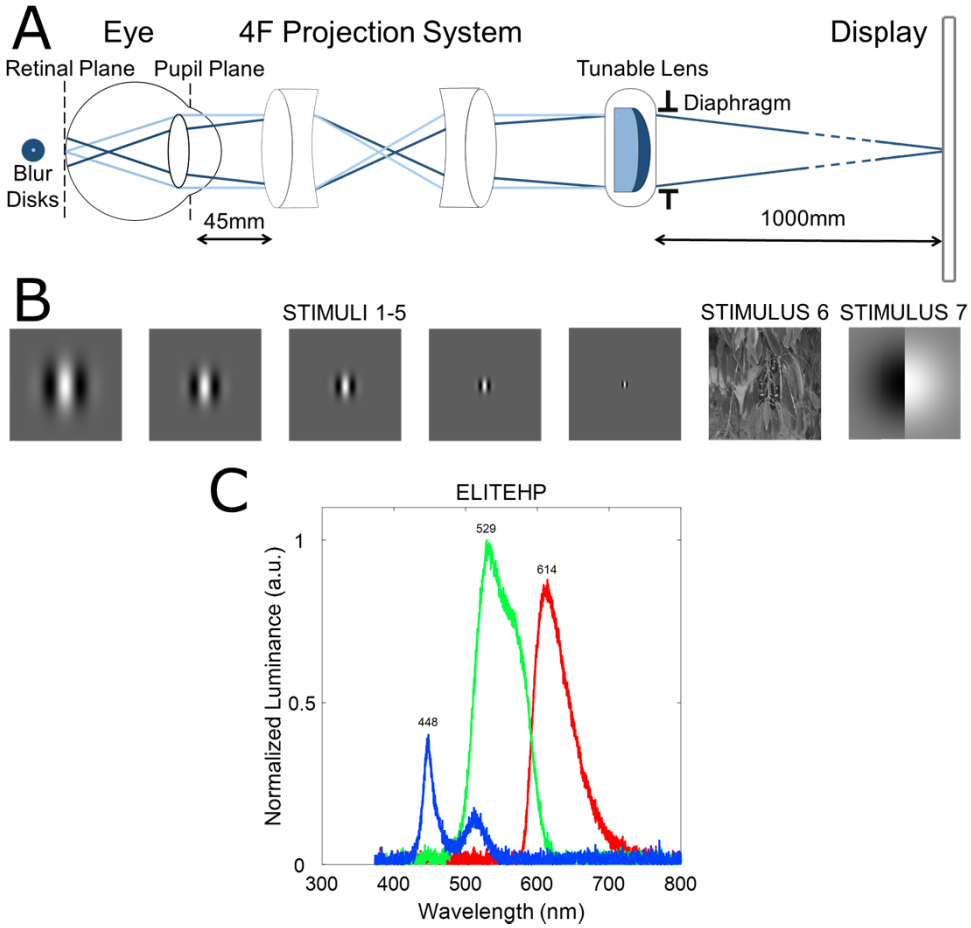

Fig. 1. Setup for the experiment. A. Schematic representation of the optical system. Retinal blur change produced by optical power change induced by the tunable lens. If the stimulus is defocused for the observer (in most situations) a large blur disk is produced on the retina (dark blue). If the tunable lens focuses the stimulus on the retina (light blue), the blur disk produced is minimum. **B. Stimuli for the experiment.** Stimuli 1-5: Gabor patches of 2, 4, 8, 16, and 32 cpd. Stimulus 6: natural image patches of vegetables, fruits, bushes, and trees subtending 4 degrees. An example of one patch is shown. Stimulus 7: gaussian edge of 0.5 degrees of standard deviation in X and Y. **C.** Normalized spectral emission of the display used in the study for the R, G, and B components. The peak of emission is also displayed.

natural images. During the experiments, all the stimuli were displayed on the monitor over a gray background.

2.4. Experiments and procedure

We used sinusoidal temporal defocus waves (sinusoidal periodic variations in optical defocus) to measure perceptual thresholds, i.e., the minimum peak-to-valley defocus (change in diopters) producing a sensation of flicker. For each stimulus (the 5 Gabor patches, the natural image, and the Gaussian edge), we measured seven testing temporal frequencies logarithmically spaced between 1.4 to 45 Hz (1.4, 2.8, 5.5, 11, 22.1, 31.3, and 44.2 Hz) in random order. The number of cycles within the interval duration (1.7 seconds, Fig. 2) was always an integer number.

Biomedical Optics EXPRESS

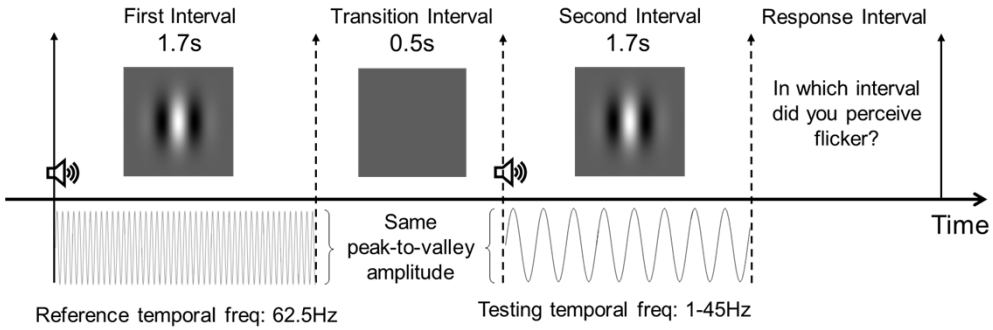

Fig. 2. Trial sequence for the experiment. For a particular condition (stimulus 1 shown as an example), reference temporal frequency is displayed in the first interval and the testing temporal frequency in the second interval (in the experiment is randomized). Miniature speakers represent sound cues. Peak-to-valley defocus change threshold is found after 30 trials.

To find the threshold, we used a Bayesian adaptive procedure (QUEST) in a two-interval forced choice (2IFC) task over 30 trials. As illustrated in Fig. 2, in each trial two different sinusoidal temporal defocus waves were induced, one as a reference with 62.5 Hz of temporal frequency and another as testing temporal frequency ranging from 1 to 45 Hz, randomly assigned to the first or the second interval. Both temporal defocus waves have the same peak-to-valley defocus change and therefore produce the same amount of retinal blur, but the reference wave is always perceived as static, and the testing wave may or may not produce detectable flicker. The reference temporal frequency of the temporal frequency was set to 62.5 Hz in all cases because i) the critical flicker frequency of the temporal contrast sensitivity function, for similar experimental luminance conditions, is always below 60 Hz [4]; and ii) pilot experiments with maximum temporal defocus wave peak-to-valley observing a laser spot providing high luminance and contrast, as well as an expanded defocus Point Spread Function (due to coherence), showed no defocus flicker perception above 50 Hz.

In each trial, the same stimulus was shown in two intervals of 1.7 seconds each. A gray screen was displayed for 0.5 seconds during a transition period between intervals. Sound cues were provided at the beginning of each interval. The task of the subject was to indicate, using a keyboard, in which of the two intervals the stimulus was perceived flickering: left-arrow for the first interval and right-arrow for the second interval.

The response was considered correct if the subject selected the testing temporal defocus wave, and incorrect if the subject selected the reference temporal defocus wave. The QUEST algorithm suggested the peak-to-valley defocus change of the next trial, based on all the previous responses of the observer. The peak-to-valley of the temporal defocus wave was changed within a range of maximum peak-to-valley change of 4.5 D (determined by the range of the tunable lens) to a minimum of 0.0 D (no change in defocus) and precision of 0.01 D. Completing each QUEST staircase took about 3 minutes.

We defined the defocus critical flicker frequency (DCFF) as the threshold separating defocus flicker perception and defocus fusion. For temporal frequencies beyond the DCFF, defocus flicker is not perceived, and the image is perceived as static. We considered that the DCFF should be calculated with a peak-to-valley defocus change of 3.0 D, the maximum defocus in a conventional visual scenario with objects at different distances: from optical infinite to near vision -considered at 33cm-.

Stimuli were generated with MATLAB (Math-works Inc., Natick, USA). Custom firmware was developed to control the electronics driving the tunable lens. PsychToolbox 3 [27] was used

Biomedical Optics EXPRESS

to synchronize the control of the tunable lens with the randomized stimulus presentation and the auditive signals, capturing the response of the subject and calculating the peak-to-valley change of the temporal defocus wave for the next iteration.

Subjects wore their optical correction to compensate for their refractive error during the experiments. The accommodation was free, except in control experiment 2. To remove acoustic cues (sounds produced by the tunable lens), subjects wore earphones and listened to music during the experiments. All subjects performed one main experiment and two control experiments.

2.4.1. Main experiment. Spatiotemporal defocus sensitivity

We measured the peak-to-valley defocus change threshold for seven temporal frequencies ranging from 1.2-45 Hz and for all stimuli (Gabor of different spatial frequencies, natural images, and edge, Fig. 1(B)). The pupil size was fixed at 4 mm.

2.4.2. Control experiment 1. Pupil size reduction

Other residual cues besides defocus introduced by the tunable lens, such as magnification or image displacement, might potentially contribute to the perception of defocus flicker. To isolate and evaluate the impact of those residual cues, we reduced the pupil size of the eye to 1 mm using a diaphragm projected onto the pupil of the eye (Fig. 1(A)), substantially reducing the retinal blur induced by defocus due to the drastic decrease of the blur disk [28], but not affecting magnifications or image displacements. The peak-to-valley defocus change threshold was then measured for the same seven temporal frequencies as in the main experiment. This control experiment was only performed for stimulus 6 (natural images, Fig. 1(B)) for all subjects.

2.4.3. Control experiment 2. Paralyzed accommodation

As accommodation was functional during the main experiment, small fluctuations of the accommodation may affect defocus flicker perception. In this control experiment, we instilled cycloplegic drugs (tropicamide 1%, second drop instilled 10 minutes after a first drop, and 30 minutes before the experiment) to paralyze the accommodation. To reduce the increase in pupil size due to the cycloplegic drugs, we kept a 4-mm pupil diameter by using a diaphragm projected onto the pupil of the eye. Control experiment 2 was carried out for stimulus 6 (natural images, Fig. 1(B)) for all subjects.

2.5. Spatiotemporal defocus sensitivity function

To fit and analyze our experimental data, we considered well-established models of contrast sensitivity. On the one hand, we used the spatial model described by Mannos et al. [29] for the spatial contrast sensitivity function (SCSF). In their model, spatial sensitivity is defined as

$$SCSF(f_s) = d\left(a + \frac{f_s}{f_{s0}}\right) e^{-\left(\frac{f_s}{f_{s0}}\right)^c}, \tag{1}$$

where f_S is the spatial frequency, d is a gain factor, a controls the shape of the curve, c determines the steepness of the curve for high frequencies and f_{s0} is the peak frequency. In our experiments, instead of luminance contrast for different spatial frequencies, we use the peak-to-valley defocus change for different spatial frequencies (shown as Gabor patches).

We define the spatial defocus sensitivity function ($SDSF(f_s)$) as the sensitivity to defocus for different spatial frequencies. To describe the $SDSF(f_s)$, we used a similar model to the one used by Mannos for the $SCSF(f_s)$ (Eq. (1)), but with different parameters (d_D, a_D, f_{s0D}, and c_D) now

Biomedical Optics EXPRESS

adapted to the presence of defocus and to the sensitivity of the observer to that defocus

$$SDSF(f_s) = d_D \left(a_D + \frac{f_s}{f_{s0D}} \right) e^{-\left(\frac{f_s}{f_{s0D}}\right)^{c_D}}. \tag{2}$$

We also considered the temporal model described by Watson for the temporal defocus sensitivity function (TCSF) [4]. The temporal sensitivity is modeled as the difference between two temporal filters, one corresponding to low temporal frequencies and the other to high temporal frequencies, modulated by a gain factor. The total filter, $ft(t)$, defines the impulse response in the temporal domain with the following equation

$$ft(t) = \varepsilon \cdot [f_1(t) - \zeta \cdot f_2(t)], \tag{3}$$

where ε is a gain factor, ζ is the transience factor, and $f_1(t)$ and $f_2(t)$ represent each filter

$$f_1(t) = u(t) \cdot (\tau \cdot (n_1 - 1)!)^{-1} \cdot \left(\frac{t}{\tau}\right)^{n_1} \cdot e^{-(t/\tau)},$$

$$f_2(t) = u(t) \cdot (\kappa \cdot \tau \cdot (n_2 - 1)!)^{-1} \cdot \left(\frac{t}{\kappa \cdot \tau}\right)^{n_2} \cdot e^{-(t/\kappa \cdot \tau)}, \tag{4}$$

where $u(t)$ is the unit step function, τ is a time constant, κ is the time constant ratio, and n is the number of stages of each filter.

Computing the Fourier transform (FT) of the impulse response (Eq. (4)), the amplitude and phase responses can be estimated in the temporal frequency domain. According to Watson [4], the amplitude response represents the temporal sensitivity ($S_T(f_t)$) of the human visual system (for luminance contrast)

$$TCSF(f_t) = FT(f(t)). \tag{5}$$

In the present study, we define for the first time the temporal defocus sensitivity function ($TDSF(f_s)$) of the human eye, as the sensitivity to defocus changes at different temporal frequencies. To describe the $TDSF(f_t)$, we used a model similar to the one used by Watson for the $TCSF(f_t)$ (Eqs. (4) and 5), but with different parameters (ε_D, ζ_D, τ_D, κ_D, n_{1D}, n_{2D}) that are now adapted to the presence of defocus and to the sensitivity of the observer to that defocus. Rearranging terms:

$$f_D(t) = \varepsilon_D u(t) \tau_D e^{-\frac{\kappa_D (t+1)}{\kappa_D \cdot \tau_D}} \cdot$$

$$\left[((n_{1D} - 1)!)^{-1} \left(\frac{t}{\tau_D}\right)^{n_{1D}} - \zeta_D (\kappa_D (n_{2D} - 1)!)^{-1} \left(\frac{t}{\kappa_D \cdot \tau_D}\right)^{n_{2D}} \right]$$

$$TDSF(f_t) = FT(f_D(t)), \tag{6}$$

where $f_D(t)$ is the total filter for defocus.

In this study, both in the spatial and temporal domains, what we actually measured was the defocus detection thresholds, which are the inverse of the defocus sensitivities. Figure 3 shows the process of fitting the models to the experimental data (only the TDSF is shown, but we used a similar approach for the SDSF). We used the Nelder-Mead simplex optimization algorithm (direct search) for each subject and stimulus, to obtain the curve of temporal defocus thresholds in D units (minimum peak-to-valley defocus change perceived) and, by inverting it, the TDSF (in D^{-1} units).

In this study, we measured combinations of the different spatial (Gabor patches) and temporal (temporal defocus changes) conditions. To construct the spatiotemporal defocus sensitivity function (STDSF), defined as the sensitivity to the presence of defocus in the spatial and temporal domain, and to compare it with the well-known spatiotemporal contrast sensitivity function (STCSF), we used the model proposed by Lambrecht et al. [30] that considers the spatiotemporal

Biomedical Optics EXPRESS

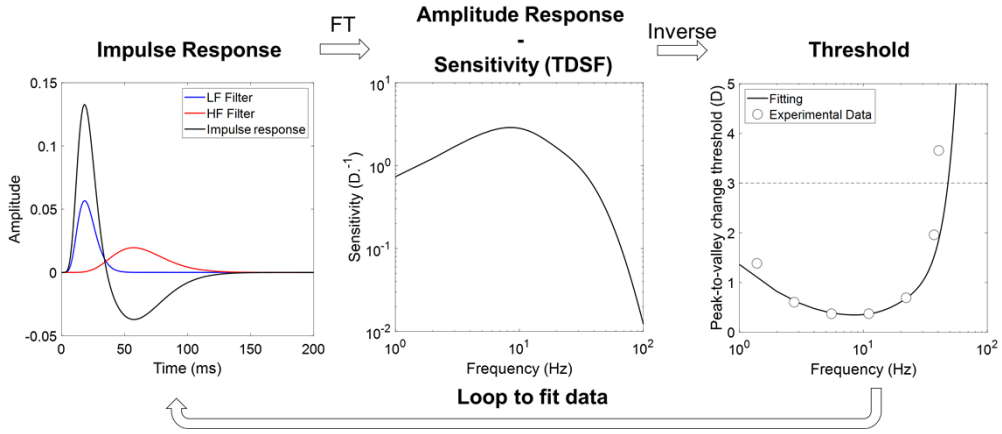

Fig. 3. Fitting model. Process of fitting the experimental data to the model described by Watson 1986 [4]. The impulse response of the system (black line in the left graph) is the difference between two filters: one for low temporal frequencies (blue line) and one for high temporal frequencies (red line). Applying a Fourier transform, we obtain the amplitude response, corresponding to the Temporal Defocus Sensitivity Function (TDSF). The inverse of the TDSF can be fitted to the experimental data.

sensitivity as a non-separable function of spatial and temporal information. According to Lambretch et al.,

$$STCSF(f_s,\, f_t) = \alpha \cdot \; (SCSF_{f_{t_1}}(f_s) \cdot TCSF_{f_{s_1}}(f_t) + \beta \cdot SCSF_{f_{t_2}}(f_s) \cdot TCSF_{f_{s_2}}(f_t)$$
$$+\gamma \cdot SCSF_{f_{t_2}}(f_s) \cdot TCSF_{f_{s_1}}(f_t) + \delta \cdot SCSF_{f_{t_1}}(f_s) \cdot TCSF_{f_{s_2}}(f_t) \tag{7}$$

where α, β, γ and δ are normalization factors, $SCSF_{f_{t_1}}$ and $SCSF_{f_{t_2}}$ are the spatial sensitivities for particular temporal frequencies (f_{t_1} and f_{t_2}) and $TCSF_{f_{s_1}}$ and $TCSF_{f_{s_2}}$ are the temporal sensitivities for particular spatial frequencies (f_{s_1} and f_{s_2}), obtained previously in Eqs. (1) and (5), respectively. In Lambretch's model, the spatial and temporal sensitivities were selected based on the original Burbeck's description [31], selecting the spatial sensitivities for 1 and 19 Hz ($SCSF_1$ and $SCSF_{19}$) and the temporal sensitivities for 0.5 and 10 cpd ($TCSF_{0.5}$ and $TCSF_{10}$). We used this same model with different parameters to describe the spatiotemporal defocus sensitivity function ($SDCSF(f_s,\, f_t)$) of the human eye

$$STDSF(f_s,\, f_t) = \alpha_D(SDSF_{f_{t_1}}(f_s) \cdot TDSF_{f_{s_1}}(f_t) + \beta_D \cdot SDSF_{f_{t_2}}(f_s)$$
$$\cdot TDSF_{f_{s_2}}(f_t) + \gamma_D \cdot SDSF_{f_{t_2}}(f_s) \cdot TDSF_{f_{s_1}}(f_t)$$
$$+\delta_D \cdot SDSF_{f_{t_1}}(f_s) \cdot TDSF_{f_{s_2}}(f_t)) \tag{8}$$

where α_D, β_D, γ_D, and δ_D are now referred to defocus sensitivity, $SDSF_{f_{t_1}}$ and $SDSF_{f_{t_2}}$ are the spatial defocus sensitivities for particular temporal frequencies (f_{t_1} and f_{t_2}) and $TDSF_{f_{s_1}}$ and $TDSF_{f_{s_2}}$ are the temporal defocus sensitivities for particular spatial frequencies (f_{s_1} and f_{s_2}), obtained previously in Eqs. (2) and (6), respectively. In our experiment, we used the spatial defocus sensitivities measured for 1.1 and 22.2 Hz and the temporal defocus sensitivities measured for 2 and 8 cpd.

The window of visibility, a concept defined for contrast sensitivity [7], describes the spatiotemporal boundary of contrast perception. Spatial and temporal components that lie outside the window are invisible, and those within the window are somewhat visible, depending on the spatiotemporal contrast sensitivity function. Similarly, we can define a window of defocus

Biomedical Optics EXPRESS

visibility, the spatiotemporal limits of defocus perception. We considered the boundary between visible and invisible when defocus sensitivity is below 0.3 D^{-1} (corresponding to a threshold defocus amplitude above 3 D, the common dioptric difference between far and near vision).

2.6. Statistical analysis

To analyze the statistical significance of the differences between stimuli (Gabor patches, natural images, and edge) and between the main experiment (for natural images) and control experiments (pupil reduction and paralyzed accommodation), paired t-tests were used. We analyzed differences for each temporal frequency measured (seven in total). The statistical level to achieve statistical significance was set to 5% ($p < 0.05$).

3. Results

Figure 4 shows a representative example of the results obtained for one subject. Figure 4(A) shows the progress of the QUEST procedure along trials for seven temporal frequencies (each one indicated with a different color) for subject 1 (S1) and a Gabor patch of 32 cpd. The peak-to-valley defocus change threshold (in D) is indicated as a dot at the end of each QUEST staircase. A peak-to-valley defocus change threshold above 3.00 D (indicated with a dashed line) is considered perception without flicker, i.e., complete fusion of the temporal defocus wave. The threshold obtained for each temporal frequency and the fitting described in Eq. (6), which represents the inverse of the Temporal Defocus Sensitivity Function (TDSF), are shown in Fig. 4(B). The minimum threshold (i.e., maximum sensitivity) and the Defocus Critical Flicker Frequency (DCFF) are indicated with a blue and red cross, respectively. For this subject and condition, flicker is not perceived at high temporal frequencies (31.2 and 44.2 Hz). The minimum threshold is 0.25 D (corresponding to a maximum sensitivity of 4.00 D^{-1}) at 11 Hz. Figure 4(C) shows the inverse of the TDSF, the DCFF, and the minimum threshold for S1 and all spatial frequencies measured. The DCFF ranged from 28 to 34 Hz and the threshold from 0.21 to 0.59 D (corresponding to maximum sensitivity of 4.76 to 1.69 D^{-1}) at 8.4 to 11.6 Hz. Overall, the DCFF is around 30 Hz, and the maximum sensitivity is around 10 Hz.

Figure 5 and Table 1 show the results averaged for all subjects and all stimuli measured. In Fig. 5(A), the results for the Gabor patches with different spatial frequencies. Similar to

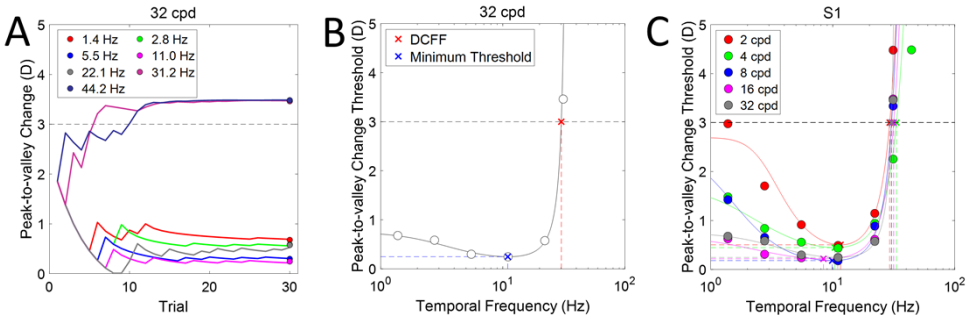

Fig. 4. Temporal sensitivity to changes in defocus. A. Progress of the Quest procedure for different temporal frequencies, for Subject S1 and a Gabor patch of 32cpd. The endpoints of each curve represent the defocus amplitude threshold estimated after 30 trials. **B.** Thresholds obtained for each temporal frequency. The black line represents the fitting of Watson's model (see Eq. (6)). Minimum threshold peak-to-valley defocus change (i.e., maximum sensitivity) is displayed as a blue cross. The Defocus Critical Flicker Frequency (DCFF) is displayed as a red cross. **C.** Thresholds were obtained for each temporal frequency and all spatial frequencies were measured for S1.

Biomedical Optics EXPRESS

the temporal sensitivity for contrast [2,32], the peak of sensitivity slightly shifts from medium temporal frequencies (10.2 and 10.5 Hz) at low temporal frequencies (2 and 4 cpd) to lower temporal frequencies (7.7 Hz) at high temporal frequencies (32 cpd). Figure 5(B) shows the results averaged across subjects for the natural images stimulus. Similarly, Fig. 5(C) shows the results averaged across subjects for the edge stimulus.

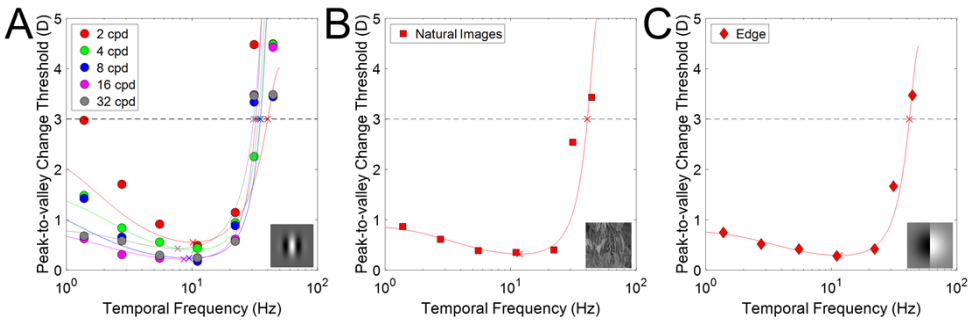

Fig. 5. Average across subjects. A miniature of each stimulus is displayed in the left corner of each subplot. **A.** Gabor patches. Defocus temporal sensitivity function for Gabor patches of different spatial frequencies. Circles represent the data and lines the fitting. Red color indicates 2 cpd, red 4 cpd, blue 8 cpd, magenta 16 cpd, and gray 32 cpd. **B.** Natural Images. Defocus temporal sensitivity function for natural images condition averaged across subjects. Red squares represent the data and the red line the fitting. **C.** Edge. Defocus temporal sensitivity function for edge condition averaged across subjects. Red diamonds represent data and the red line represents the fitting.

Table 1. Temporal sensitivity function results for all stimuli. Minimum threshold, maximum sensitivity, temporal frequency at maximum sensitivity, and defocus critical flicker frequency averaged across subjects.

Stimulus	Minimum threshold (D)	Maximum sensitivity (D^{-1})	Temporal frequency maximum (Hz)	DCFF (Hz)
Gabor 2 cpd	0.55	1.81	10.2	40
Gabor 4 cpd	0.40	2.50	10.5	33.7
Gabor 8 cpd	0.25	4.00	9.4	32.3
Gabor 16 cpd	0.22	4.54	8.6	32.2
Gabor 32 cpd	0.43	2.33	7.7	31
Natural Image	0.32	3.13	11.8	40.9
Edge	0.29	3.44	11.6	41.9
Average across stimulus	0.35 ± 0.11	3.11 ± 0.97	9.97 ± 1.51	36.0 ± 4.7
Reduced pupil	0.50	2.00	3.6	22.3
Paralyzed accommodation	0.34	2.94	7.0	36.1

Comparing the Gabor of spatial frequency with maximum sensitivity (16 cpd) with natural images and edge stimulus, no significant differences are found for any temporal frequency (paired t-test $p < 0.05$ in all comparisons).

3.1. Control experiments

Figure 6 shows the results of the natural image stimulus averaged across all subjects for the normal experiment (in red), for the control experiment 1 (pupil reduction, in green), and for the

Biomedical Optics EXPRESS

control experiment 2 (paralyzed accommodation, in dark yellow). For pupil reduction, the DCFF is found at 22.3 Hz and the minimum threshold found is 0.50 D (2.00 D^{-1}) at 3.6 Hz (see Table 1). Although the threshold is slightly lower for low temporal frequencies 1.4 and 2.8 Hz, paired t-tests do not find significant differences for these low temporal frequencies ($p > .05$). For higher temporal frequencies above 2.8 Hz, thresholds are significantly higher ($p < .05$, and therefore sensitivity lower).

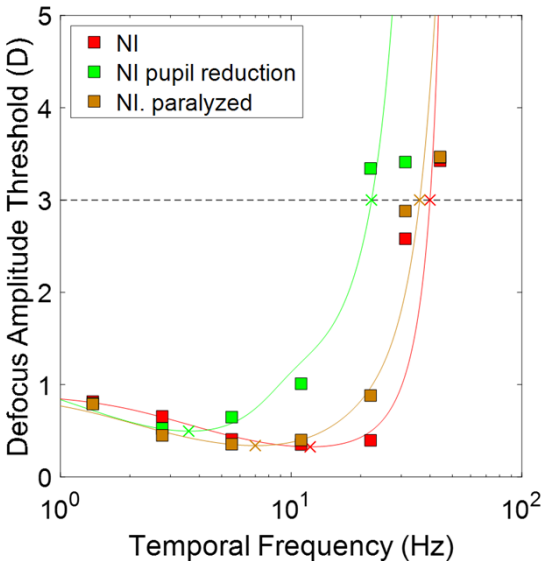

Fig. 6. Control experiments. Results for the main experiment for natural image stimulus (abbreviated as NI) and the control experiments. In red, the main experiment, in green control experiment 1 (pupil reduction), and in dark yellow control experiment 2 (paralyzed accommodation).

For the paralyzed accommodation control experiment, the DCFF is found at 36.1 Hz and the minimum threshold is found at 0.34 D (2.94 D^{-1}) at 7 Hz, (Table 1). For control experiment 2, paired t-tests report non-significant differences for any temporal frequencies ($p < .05$), suggesting that accommodation does not influence the flicker detection task.

3.2. Spatial defocus sensitivity function

To estimate the spatial defocus sensitivity function (SDSF) we fit the equations described in the *Methods* section and developed by Mannos et al. [29]. The results averaged across subjects are shown in Table 2 and plotted in Fig. 7(A) (left plot). We do not show the results for 44.4 Hz because experimental thresholds were above 3.0 D for all temporal frequencies and all subjects. Interestingly, the peak of sensitivity shifts from high spatial frequencies (21 cpd) at low temporal frequencies (1.4 Hz) to medium/low spatial frequencies (6 cpd) at high temporal frequencies (31.2 Hz). Besides, the sensitivity for 22.1 and 31.2 Hz decreases at all spatial frequencies and the curves follow slightly different trends. These results are in agreement with the results found by others for contrast sensitivity [2,32,33].

3.3. Spatiotemporal defocus sensitivity function

To obtain the SDSF (Fig. 7(A), left plot), the TDSF (Fig. 7(A), middle plot), and the spatiotemporal defocus sensitivity function (STDSF, Fig. 7(A), right plot) we used Eq. (2), Eq. (6), and Eq. (8), respectively. The parameters of the model fitting the STDSF (Fig. 7(A); right plot) where α_D=1,

Biomedical Optics EXPRESS

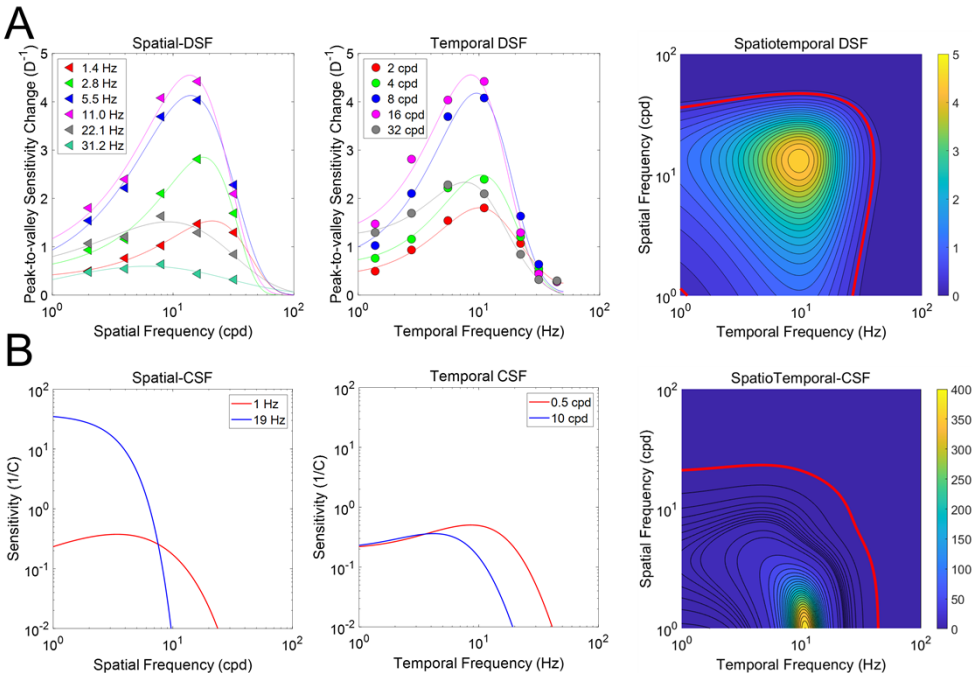

Fig. 7. Spatiotemporal Sensitivity. A. Spatiotemporal Defocus Sensitivity Function (STDSF). Spatiotemporal defocus sensitivity function from the experimental data obtained in this study, averaged across subjects and conditions. On the left, the spatial defocus sensitivity function (SDSF) for different temporal frequencies. In the middle, the temporal defocus sensitivity function (TDSF) for different spatial frequencies. On the left, the spatiotemporal defocus sensitivity function (STDSF) contour plot. In red, the defocus window of visibility. **B. Spatiotemporal Contrast Sensitivity Function (SCDSF).** On the left, the spatial contrast sensitivity function (SCSF) for 19 and 1 Hz temporal frequencies, based on Mannos et al. [29]. In the middle, the temporal contrast sensitivity function (TCSF) for 10 and 0.5 cpd spatial frequencies, based on Watson [4]. On the right, the spatiotemporal contrast sensitivity function (STCSF), based on Lambretch et al. [30].

Table 2. Spatial sensitivity function results for all stimuli. Minimum threshold, maximum sensitivity, temporal frequency at maximum sensitivity, and defocus critical flicker frequency averaged across subjects.

Temporal Frequency (Hz)	Minimum threshold (D)	Maximum sensitivity (D^{-1})	Spatial frequency maximum (cpd)	DCFF (cpd)
1.4	0.65	1.54	21.0	57.6
2.8	0.35	2.86	17.8	47.8
5.5	0.24	4.17	14.0	58.8
11.0	0.22	4.55	13.8	51.4
22.1	0.66	1.51	9.0	56.0
31.2	0.60	1.67	6.0	28.8

β_D=10, γ_D=-5, and δ_D=3.74. The maximum sensitivity is 4.55 D^{-1} (0.22 D) and is found at 13.6 cpd and 9.6 Hz. The window of visibility for defocus (displayed as a red line) is defined as the boundaries for defocus perception and is found when sensitivity decreases to 0.3 D^{-1} (inverse of 3.0 D), covering a region around 40 cpd to 40 Hz. Table 3 shows the parameters of the SDSF

Biomedical Optics EXPRESS

for all temporal frequencies and the parameters of the TDSF for all spatial frequencies, shown in Fig. 7(A).

Table 3. Parameters of the models for SDSF and TDSF. The data for the fitting was obtained from the averages across subjects for the Gabor stimuli.

$SDSF(f_t)$				
Temporal Frequency (Hz)	d_D	a_D	f_{s0D}	c_D
1.38	3.27	0.01	31.36	1.77
2.76	5.89	0.07	26.51	2.13
5.52	10.53	0.03	17.4	1.27
11.05	10.76	0.06	18.99	1.51
22.10	3.40	0.14	5.62	0.67
31.25	0.61	-0.54	0.36	0.37

$TDSF(f_s)$						
Spatial Frequency (cpd)	ε_D	ζ_D	τ_D	κ_D	n_{1D}	n_{2D}
2	2.05	0.81	6.6	0.43	8	9
4	20.81	0.97	5.52	0.93	9	9
8	49.81	0.99	6.47	0.84	8	9
16	13.89	0.91	7.25	0.71	9	10
32	3.22	0.62	8.17	0.45	8	9

For comparison purposes, Fig. 7(B) shows the spatiotemporal sensitivity to just noticeable luminance variations (contrast), the spatial contrast sensitivity function (SCSF, left plot), temporal contrast sensitivity function (TCSF, middle plot), and spatiotemporal contrast sensitivity function, (STCSF, right plot). For the STCSF the maximum is 385 (0.0026 contrast threshold) at around 1 cpd and 10 Hz. The window of visibility for contrast (displayed also as a red line) is found when contrast sensitivity decreases to 1 (inverse of 3.0 D), covering a region around 30 cpd to 60 Hz.

4. Discussion

4.1. Spatiotemporal defocus sensitivity function

In this study, we have measured and described, for the first time, the spatiotemporal defocus sensitivity function (STDSF). Our results report, on average across subjects, a maximum in the sensitivity to changes in defocus at 13.6 cpd and 9.6 Hz. In comparison, the maximum of the spatiotemporal contrast sensitivity function (STCSF), has been reported to appear at very different spatial frequencies (1-2 cpd) and similar temporal frequencies (10 Hz). The shapes of both sensitivity surfaces follow the same trend, although the peak of the STDSF is centered, and the peak of the STCSF is shifted toward lower frequencies (from 14 cpd in defocus, to 2 cpd in contrast). In other words, modulations in defocus cause bigger (more visible) changes in contrast at high spatial frequencies than at low spatial frequencies. The absolute value of maximum sensitivity is much higher for contrast than for defocus (385 vs 0.45 D^{-1}), but this is due to the different magnitudes and units involved (contrast vs diopters).

The maximum sensitivity found for the spatiotemporal defocus sensitivity is 0.45 D^{-1}, equivalent to a threshold of 0.22 D. This result is similar to the threshold measured by other authors, which reported a threshold to defocus around 0.2 D [34,35]. However, the comparison of this first study of the spatiotemporal defocus sensitivity with those of the literature is not

Biomedical Optics EXPRESS

straightforward: defocus in those studies was static, the stimulus was a letter instead of Gabor patches, and the population included myopic and emmetropic adults [34] or myopic kids [35].

The model described by Watson [4] to explain the temporal contrast sensitivity function (TCSF) was adapted in this study to fit the temporal defocus sensitivity function (TDSF). When using the model with our experimental data and the new magnitude (defocus), we obtained different results than those obtained with contrast. First, in Watson's model, the contrast critical flicker frequency (CFF) varied between 50-70 Hz, depending on the stimulus condition. However, our data yields defocus critical flicker frequencies (DCFFs) around 30-40 Hz using a high-contrast stimulus. It is noticeable that while the CFF is obtained with the maximum physical contrast (~1), the DCFF is obtained here at ~3.0 D of defocus, a relatively low limit for defocus changes, defined as the dioptric change between far and near vision (3.0 D). A higher dioptric limit may have shifted the DCFF to higher temporal frequencies, but 3.0 D seems like a reasonable limit in vision as larger defocus changes are unusual.

Mannos et al. [29] described a model for spatial contrast sensitivity that was used in this study to find the spatial defocus sensitivity function (SDSF). After fitting, the model predicted our experimental data well. In addition, the model proposed by Burbeck et al. [31] and lately refined by Lambrecht et al. [30] was also used to describe the STDSF.

In this study, we used constant-cycles Gabor patches, that maintained the shape of the stimulus and the number of cycles across spatial frequencies but varied the size of the Gabor. It has been reported that constant-cycle Gabors (like the ones used in this study) are less sensitive than constant-degree Gabors (which keep the size but vary the number of cycles) to changes in contrast [36]. However, constant-cycle Gabors are used to model ideal observers and are potentially more useful than constant-degree Gabors to model real work performance in natural images. After this careful analysis, we decided to scale the full stimulus up and down, keeping the stimulus shape and the number of cycles constant while changing the spatial frequency. Nevertheless, further studies should address measurements using constant-degree Gabors and other stimuli, to provide a more complete description of the spatiotemporal defocus sensitivity function.

As mentioned in the introduction, other authors have measured the sensitivity to defocus changes but induced onscreen by filtering an edge with a Gaussian filter [17]. However, optical blur is different from a Gaussian, as optical aberrations of the eye, especially high-order aberrations, are combined with defocus [8]. We used optical defocus in this study for two reasons: i) Optical defocus is more natural than onscreen blur; and ii) this study was motivated by applications where actual changes in optical defocus are applied, like temporal multiplexing in visual simulations [19]. A future study could address the differences between onscreen and optical blur in the spatiotemporal defocus sensitivity function while measuring the optical aberrations of the human eye to account for their effect on the defocus sensitivity.

4.2. Influence of the pupil

For the control experiment 1, with reduced pupil diameter, the sensitivity at medium and high temporal frequencies (>2.8 Hz) was significantly lower (higher threshold, Fig. 6) than for the normal experiment. By reducing the pupil size, the goal was to minimize (not completely remove) defocus as a cue while keeping other effects that might be contributing to the detection of flicker. We expected an increase in the threshold (decrease in sensitivity), and that is what we report. This result can be explained by the large overall reduction in retinal blur and the increase in depth-of-focus due to pupil reduction [28], which effectively reduces the differences in the retinal image with the different defocus levels, and therefore the sensation of flicker.

4.3. Defocus flicker-detection task and accommodation

A physiological source of temporal changes in defocus is accommodation, the ability of the crystalline lens to change its optical power. Accommodation could be a very fast process, that

Biomedical Optics EXPRESS

can be activated in 300 ms [37]. However, it has also been reported that the accommodative system is not able to follow changes in defocus faster than 2 Hz [10–16]. Beyond that frequency, the temporal response of accommodation is erratic and hardly accurate. Other studies have reported fluctuations in the accommodation response as high as 0.5 D with flickering stimuli at different temporal frequencies, ranging from 0.5 up to 20 Hz [38–42]. This fluctuation occurs in a blur-detection task, where the accommodation is elicited on purpose for focusing on the target. The reason why we believe that accommodation is not playing a role in these measurements is that, in our study, the task was to detect defocus flicker and not to keep the image sharp while changing the focus, and therefore the accommodation system is not forced. In control experiment 2, where the accommodation was paralyzed by instilling cycloplegic drugs, we found slightly higher sensitivities at low temporal frequencies than in the normal experiment with free accommodation (Fig. 6), but the differences were not statistically significant. Besides, in the same control experiment for medium and high temporal frequencies, the results are statistically similar. Both results suggest that accommodation does not vary during the defocus flicker sensitivity, even at low temporal frequencies. The varying defocus seems to deactivate accommodation, and the eye keeps its optical power stable, probably in a relaxed position. Nevertheless, in further research, we should directly measure the behavior of the accommodation specifically in a defocus flicker-detection task to yield proper conclusions about the state of the accommodation.

Another interesting point is that the sensitivity to changes in defocus is best when the eye is slightly out of focus [10]. In our paradigm, we measured the spatiotemporal sensitivity to defocus in subjects where the eye is presumably in good focus as subjects wore their far prescription during the measurements, and therefore sensitivity may vary by shifting the mean position of the temporal defocus wave. Further studies could address this question.

4.4. Clinical implications of the spatiotemporal defocus sensitivity function

The STDSF does not only provide basic scientific knowledge but a theoretical framework for new technologies that make use of temporal changes in defocus. SimVis Gekko is a visual simulator that uses tunable lenses under a temporal multiplexing approach. It induces fast changes in defocus to project onto the retina of the patient a superposition of image components that are perceived as a static multifocal image, thanks to temporal fusion. In this way, the device can provide programmable simulations of existing multifocal lens models. SimVis Gekko works at a temporal frequency of 50 Hz [19,43], above all the defocus critical flicker frequencies measured in this study for all conditions, and therefore defocus flicker should not be perceived with the instrument. Moreover, the temporal sensitivity to contrast decreases with age, with a shift of the maximum sensitivity to lower temporal frequencies [44]. Further studies of defocus flicker might include presbyopes, the target for multifocal corrections, and SimVis Gekko.

Another recent application using fast changes in defocus is direct subjective refraction (DSR). It is a new method for estimating the refractive error of an eye, which uses temporal changes in defocus of 15 Hz to elicit chromatic flicker cues on purpose on a bichromatic stimulus and to find the spherical equivalent of the eye [20]. The results of the present study can be used to derive the optimal parameters for this new visual task and for selecting the temporal defocus change to use in the method.

5. Conclusions

In this study we have reported for the first time the spatiotemporal defocus sensitivity function of the human eye, finding a maximum of sensitivity around 14 cpd and 10 Hz (spatial frequency and temporal frequency) and the upper limits of the window of defocus sensitivity at 40 cpd and 40 Hz. We have also demonstrated that accommodation remains in a fixed state while performing a defocus flicker-detection task. The spatiotemporal defocus sensitivity function has implications for new technologies whose working principles make use of fast changes in defocus.

Biomedical Optics EXPRESS

Funding. "la Caixa" Foundation (ID 100010434; LCF/BQ/DR19/11740032); Ministerio de Educación y Formación Profesional (FPU17/02760); National Institutes of Health (EY02466, EY11747); Ministerio de Ciencia, Innovación y Universidades (FIS2017-84753-R, ISCIII DTS2016/00127).

Acknowledgments. We thank Dr. Johannes Burge for his excellent support in the development of the Gabor stimuli.

Disclosures. Not applicable.

Data Availability. Data underlying the results presented in this paper are not publicly available at this time but may be obtained from the authors upon reasonable request.

References

1. H. de Lange Dzn, "Research into the dynamic nature of the human fovea-cortex systems with intermittent and modulated light. I. Attenuation characteristics with white and colored light," J. Opt. Soc. Am. **48**(11), 777–784 (1958).
2. J. G. Robson, "Spatial and temporal contrast-sensitivity functions of the visual system," J. Opt. Soc. Am. **56**(8), 1141 (1966).
3. F. L. van Nes, J. J. Koenderink, H. Nas, and M. A. Bouman, "Spatiotemporal modulation transfer in the human eye," J. Opt. Soc. Am. **57**(9), 1082–1088 (1967).
4. A. B. Watson, "Temporal Sensitivity," in *Handbook of Perception and Human Performance* (Wiley, 1986), Chapt. 6, 6:1–6:43.
5. C. Owsley, "Contrast sensitivity," Ophthalmol. Clin. North Am. **16**(2), 171–177 (2003).
6. D. G. Pelli and P. Bex, "Measuring contrast sensitivity," Vision Res. **90**, 10–14 (2013).
7. A. B. Watson, A. Ahumada, and J. E. Farrell, "Window of Visibility: a psychophysical theory of fidelity in time-sampled visual motion displays," J. Opt. Soc. Am. A **3**(3), 300–307 (1986).
8. A. B. Watson and A. J. Ahumada, "Blur clarified: A review and synthesis of blur discrimination," J. Vis. **11**(5), 10 (2011).
9. J. Burge and W. S. Geisler, "Optimal defocus estimation in individual natural images," Proc. Natl. Acad. Sci. U. S. A. **108**(40), 16849–16854 (2011).
10. F. W. Campbell and G. Westheimer, "Sensitivity of the eye to differences in focus," J. Physiol. **143**, 18P (1958).
11. F. W. Campbell, J. G. Robson, and G. Westheimer, "Fluctuations of accommodation under steady viewing conditions," J. Physiol. **145**(3), 579–594 (1959).
12. V. V. Krishnan, S. Phillips, and L. Stark, "Frequency analysis of accommodation, accommodative vergence and disparity vergence," Vision Res. **13**(8), 1545–1554 (1973).
13. C. M. Schor and J. C. Kotulak, "Dynamic interactions between accommodation and convergence are velocity sensitive," Vision Res. **26**(6), 927–942 (1986).
14. F. Sun, L. Stark, A. N. Nguyen, J. Wong, V. Lakshminaryanan, and E. Mueller, "Changes in Accommodation with Age: Static and Dynamic," Optom. Vis. Sci. **65**(6), 492–498 (1988).
15. G. Walsh and W. N. Charman, "Visual sensitivity to temporal change in focus and its relevance to the accommodation response," Vision Res. **28**(11), 1207–1221 (1988).
16. S. Mathews and P. B. Kruger, "Spatiotemporal transfer function of human accommodation," Vision Res. **34**(15), 1965–1980 (1994).
17. A. C. Bilson, Y. Mizokami, and M. A. Webster, "Visual adjustments to temporal blur," J. Opt. Soc. Am. A **22**(10), 2281 (2005).
18. C. Dorronsoro, X. Barcala, E. Gambra, V. Akondi, L. Sawides, Y. Marrakchi, V. Rodriguez-Lopez, C. Benedi-Garcia, M. Vinas, E. Lage, and S. Marcos, "Tunable lenses: Dynamic characterization and fine-tuned control for high-speed applications," Opt. Express **27**(3), 2085–2100 (2019).
19. C. Dorronsoro, A. Radhakrishnan, J. R. Alonso-Sanz, D. Pascual, M. Velasco-Ocana, P. Perez-Merino, and S. Marcos, "Portable simultaneous vision device to simulate multifocal corrections," Optica **3**(8), 918–924 (2016).
20. V. Rodriguez-Lopez, A. Hernandez-Poyatos, and C. Dorronsoro, "The Direct Subjective Refraction: Unsupervised measurements of the subjective refraction using defocus waves," bioRxiv, 2021.12.04.471123 (2021).
21. X. Barcala, E. Gambra, L. Sawides, I. Martinez-Ibarburu, V. Rodriguez-Lopez, and C. Dorronsoro, "Optical quality evaluation for active afocal systems," Proc. SPIE **11871**, 118710Q (2021).
22. A. G. Lopez-de-Haro, X. Barcala, I. Martinez-Ibarburu, Y. Marrakchi, E. Gambra, V. Rodriguez-Lopez, L. Sawides, and C. Dorronsoro, "Closed-loop experimental optimization of tunable lenses," Appl. Opt. **61**(27), 8091–8099 (2022).
23. Y. Marrakchi, X. Barcala, E. Gambra, I. Martinez-Ibarburu, C. Dorronsoro, and L. Sawides, "Experimental characterization, modelling and compensation of temperature effects in optotunable lenses," Sci. Rep. **13**(1), 1575 (2023).
24. M. Vinas, C. Dorronsoro, A. Radhakrishnan, C. Benedi-Garcia, E. A. LaVilla, J. Schwiegerling, and S. Marcos, "Comparison of vision through surface modulated and spatial light modulated multifocal optics," Biomed. Opt. Express **8**(4), 2055–2068 (2017).
25. M. Vinas, C. Benedi-Garcia, S. Aissati, D. Pascual, V. Akondi, C. Dorronsoro, and S. Marcos, "Visual simulators replicate vision with multifocal lenses," Sci. Rep. **9**(1), 1539 (2019).

Biomedical Optics EXPRESS

26. J. Vazquez, C. A. Párraga, R. Baldrich, and V. Maria, "Color constancy algorithms: Psychophysical evaluation on a new dataset," J. Imaging Sci. Technol. **53**(3), 31105-1–31105-9 (2009).
27. D. H. Brainard, "The Psychophysics Toolbox," Spat. Vis. **10**(4), 433–436 (1997).
28. A. Roorda and D. R. Williams, "The arrangement of the three cone classes in the living human eye," Nature **397**(6719), 520–522 (1999).
29. J. L. Mannos and D. J. Sakrison, "The effects of a visual fidelity criterion on the encoding of images," IEEE Trans. Inf. Theory **20**(4), 525–536 (1974).
30. C. J. van den Branden, V. D. B. Lambrecht, and M. Kunt, "Characterization of human visual sensitivity for video imaging applications," Signal Processing **67**(3), 255–269 (1998).
31. C. A. Burbeck and D. H. Kelly, "Spatiotemporal characteristics of visual mechanisms: excitatory-inhibitory model," J. Opt. Soc. Am. **70**(9), 1121–1126 (1980).
32. D. H. Kelly, "Retinal inhomogeneity. I. Spatiotemporal contrast sensitivity," J. Opt. Soc. Am. A **1**(1), 107–113 (1984).
33. M. J. Wright and A. Johnston, "Spatiotemporal contrast sensitivity and visual field locus," Vision Res. **23**(10), 983–989 (1983).
34. M. Rosenfield and J. A. Abraham-Cohen, "Blur Sensitivity in Myopes," Optom. Vis. Sci. **76**(5), 303–307 (1999).
35. K. L. Schmid, D. Robert Iskander, R. W. H. Li, M. H. Edwards, and J. K. F. Lew, "Blur detection thresholds in childhood myopia: single and dual target presentation," Vision Res. **42**(2), 239–247 (2002).
36. A. B. Watson, "The field of view, the field of resolution, and the field of contrast sensitivity," J. Percept. Imaging **1**(1), 10505-1–10505-11 (2018).
37. N. Sharmin and B. Vohnsen, "Monocular accommodation response to random defocus changes induced by a tuneable lens," Vision Res. **165**, 45–53 (2019).
38. C. Neary, "The effect of high frequency flicker on accommodation," Ophthalmic Physiol. Opt. **9**(4), 440–446 (1989).
39. D. I. Flitcroft, "Accommodation and flicker: evidence of a role for temporal cues in accommodation control?" Ophthalmic Physiol. Opt. **11**(1), 81–90 (1991).
40. C. a. Charman, "Accommodation responses to flickering stimuli," Ophthalmic Physiol. Opt. **16**(5), 391–408 (1996).
41. W. N. Charman and G. Heron, "Microfluctuations in accommodation: An update on their characteristics and possible role," Ophthalmic Physiol. Opt. **35**(5), 476–499 (2015).
42. L. Zhang, D. Guo, C. Xie, Y. Wen, X. Zhang, L. Jin, J. Tong, and Y. Shen, "The effects of colour and temporal frequency of flickering light on variability of the accommodation response in emmetropes and myopes," BMC Ophthalmol. **21**(1), 88 (2021).
43. X. Barcala, M. Vinas, M. Romero, E. Gambra, J. Luis, M. Gonzalez, S. Marcos, and C. Dorronsoro, "Multifocal acceptance score to evaluate vision: MAS - 2 EV," Sci. Rep. **11**(1), 1397 (2021).
44. C. W. Tyler, "Two processes control variations in flicker sensitivity over the life span," J. Opt. Soc. Am. A **6**(4), 481–490 (1989).